AD-A154 376 NITROGEN CHEMISTRY IN SEA LEVEL AIR FOLLOWING LARGE RADIATION DOSES(U) MISSION RESEARCH CORP SANTA BARBARA CA M SCHEIBE 15 JUN 84 MRC-R-845 DNA-TR-84-307 1/1

UNCLASSIFIED DNA001-80-C-0151 F/G 7/5 NL

END

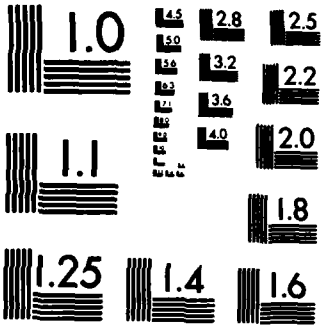

MICROCOPY RESOLUTION TEST CHART
NATIONAL BUREAU OF STANDARDS-1963-A

AD-A154 376

DNA-TR-84-307

NITROGEN CHEMISTRY IN SEA LEVEL AIR FOLLOWING LARGE RADIATION DOSES

Murray Scheibe
Mission Research Corp
P.O. Drawer 719
Santa Barbara, CA 93102-0719

15 June 1984

Technical Report

CONTRACT No. DNA 001-80-C-0151

APPROVED FOR PUBLIC RELEASE;
DISTRIBUTION UNLIMITED.

THIS WORK WAS SPONSORED BY THE DEFENSE NUCLEAR AGENCY
UNDER RDT&E RMSS CODE B322081466 S99QAXHD00004 H2590D.

DTIC FILE COPY

Prepared for
Director
DEFENSE NUCLEAR AGENCY
Washington, DC 20305-1000

DTIC
ELECTE
JUN 3 1985
S D
B

85 03 29 016

Destroy this report when it is no longer needed. Do not return to sender.

PLEASE NOTIFY THE DEFENSE NUCLEAR AGENCY, ATTN: STTI, WASHINGTON, DC 20305-1000, IF YOUR ADDRESS IS INCORRECT, IF YOU WISH IT DELETED FROM THE DISTRIBUTION LIST, OR IF THE ADDRESSEE IS NO LONGER EMPLOYED BY YOUR ORGANIZATION.

UNCLASSIFIED
SECURITY CLASSIFICATION OF THIS PAGE

REPORT DOCUMENTATION PAGE

1a. REPORT SECURITY CLASSIFICATION UNCLASSIFIED	1b. RESTRICTIVE MARKINGS
2a. SECURITY CLASSIFICATION AUTHORITY	3. DISTRIBUTION/AVAILABILITY OF REPORT Approved for public release; distribution is unlimited.
2b. DECLASSIFICATION/DOWNGRADING SCHEDULE	
4. PERFORMING ORGANIZATION REPORT NUMBER(S) MRC-R-845	5. MONITORING ORGANIZATION REPORT NUMBER(S) DNA-TR-84-307
6a. NAME OF PERFORMING ORGANIZATION Mission Research Corporation 6b. OFFICE SYMBOL (If applicable)	7a. NAME OF MONITORING ORGANIZATION Director Defense Nuclear Agency
6c. ADDRESS (City, State, and ZIP Code) P. O. Drawer 719 Santa Barbara, CA 93102-0719	7b. ADDRESS (City, State, and ZIP Code) Washington, DC 20305-1000
8a. NAME OF FUNDING/SPONSORING ORGANIZATION 8b. OFFICE SYMBOL (If applicable)	9. PROCUREMENT INSTRUMENT IDENTIFICATION NUMBER DNA 001-80-C-0151
8c. ADDRESS (City, State, and ZIP Code)	10. SOURCE OF FUNDING NUMBERS

PROGRAM ELEMENT NO	PROJECT NO	TASK NO	WORK UNIT ACCESSION NO
62715H	S99QAXH	D	DH005185

11. TITLE (Include Security Classification)

NITROGEN CHEMISTRY IN SEA LEVEL AIR FOLLOWING LARGE RADIATION DOSES

12. PERSONAL AUTHOR(S)
Murray Scheibe

13a. TYPE OF REPORT	13b. TIME COVERED	14. DATE OF REPORT (Year, Month, Day)	15. PAGE COUNT
Technical	FROM 80Feb01 TO 81Sep30	1984 June 15	40

16. SUPPLEMENTARY NOTATION
This work was sponsored by the Defense Nuclear Agency under RDT&E RMSS Code B322081466 S99QAXHD00004 H2590D.

17. COSATI CODES			18. SUBJECT TERMS (Continue on reverse if necessary and identify by block number)
FIELD	GROUP	SUB-GROUP	Nuclear Burst, Radiation Chemistry, Nitric Acid, Bomblight, Nitrous Oxide
4	1		
6	18		

19. ABSTRACT (Continue on reverse if necessary and identify by block number)

The electron densities near a large yield nuclear burst during the first few seconds can impact the performance of terminal defense radars. The main chemical parameters which determine the electron density in this situation are the electron attachment and detachment rates. This report describes work done to determine the production of HNO_3 and N_2O, good attachers of electrons, by the burst radiation and the effect on electron detachment caused by bomblight induced photochemical reactions.

In the matter of the production of HNO_3 and N_2O the results of an experiment done at Oak Ridge were used to revise the reaction scheme used in the chemical integration code used to simulate the nuclear case. It was found that the irradiation time is a critical factor in the production of HNO_3. An order of magnitude or more less HNO_3 was produced

20. DISTRIBUTION/AVAILABILITY OF ABSTRACT ☐ UNCLASSIFIED/UNLIMITED ☒ SAME AS RPT ☐ DTIC USERS	21. ABSTRACT SECURITY CLASSIFICATION UNCLASSIFIED
22a. NAME OF RESPONSIBLE INDIVIDUAL Betty L. Fox	22b. TELEPHONE (Include Area Code) (202) 325-7042 / 22c. OFFICE SYMBOL DNA/STTI

DD FORM 1473, 84 MAR — 83 APR edition may be used until exhausted. All other editions are obsolete.

SECURITY CLASSIFICATION OF THIS PAGE
UNCLASSIFIED

19. ABSTRACT (continued)

in the nuclear cases simulated than in the laboratory experiment where the irradiation times were longer. HNO_3, however might still be an important attacher of electrons in the nuclear case.

The bomblight does not appear to affect very strongly the electron densities in the air outside the fireball. The delayed gamma-ray radiation tends to overwhelm the bomblight effect.

TABLE OF CONTENTS

Section		Page
1	INTRODUCTION	1
2	RADIATION INDUCED NITROGEN AND HYDROGEN CHEMISTRY	3
3	OAK RIDGE EXPERIMENT	8
4	ION-ION RECOMBINATION	10
5	NO_2 NEUTRAL CLUSTERS	12
6	CALCULATIONAL SIMULATION OF EXPERIMENT	14
7	NUCLEAR EFFECTS CALCULATIONS	18
8	BOMBLIGHT EFFECTS	22
9	CONCLUSIONS	26
	REFERENCES	27

Accession For
NTIS GRA&I ☑
DTIC TAB ☐
Unannounced ☐
Justification
By
Distribution/
Availability Codes
Dist | Avail and/or Special
A-1

DTIC COPY INSPECTED 3

SECTION 1
INTRODUCTION

The electron densities near a large yield nuclear burst (i.e., within about one fireball radius) during the first few seconds can impact the performance of terminal defense radars. The main chemical parameters which determine the electron density in this situation are the electron attachment and detachment rates.

The photochemical process caused by bomblight are poorly understood and we thought that these mechanisms might increase the electron density at the time of thermal maximum sufficiently to degrade these radars. Increased attachment on the other hand would decrease the electron density and could be caused by species which are produced by the high energy radiation emanating from the nuclear weapon (X-rays, neutrons, gamma rays). The production of long lived species, such as NO, NO_2, HNO_2, HNO_3 and N_2O is not, as yet, well understood. In particular HNO_3 and, under certain conditions, N_2O are known to be efficient attachers of electrons.

In the work covered in this report we have attempted to determine the production of HNO_3 and N_2O in the nuclear case. In this work we used the results from an Oak Ridge experiment to be described to improve the chemistry scheme in our computer code.

The first section which follows will describe the nitrogen and hydrogen chemistry governing the production of HNO_3 and N_2O. The next section describes the Oak Ridge experiment and its results. The following

two sections describe the revisions made to our chemistry code to increase agreement between the code and the experiment. The next section shows the results predicted by our code when simulating the experiment and the degree of agreement and the following section describes the results of the revised code in simulation of a nuclear burst. The next to the last section describes our efforts to calculate the effects of photodetachment and photodissociation on the electron densities near a burst. The result of this was negative. The final section contains our conclusions.

SECTION 2
RADIATION INDUCED NITROGEN AND HYDROGEN CHEMISTRY

The production of long lived nitrogen minor species is initiated by the deposition in the surrounding air of the high energy radiation from the nuclear weapon. The degradation of this energy is accompanied by the production, in addition to electron and ions, of species not normally found in ambient air in appreciable quantities. Table 1 contains a list of these species and the yields per ion pair. Also listed is the ion distribution. These numbers represent the best estimate[1,2] but have considerable uncertainties associated with them.

Table 1. Species production per ion-pair.

N_2^+	0.63
O_2^+	0.16
N^+	0.14
O^+	0.07
$N_2(A)$	0.60
$O_2(^1\Delta)$	0.30
$O_2(^1\Sigma)$	0.10
$O(^3P)$	0.21
$O(^1D)$	0.12
$N(^4S)$	0.60
$N(^2D)$	0.64

The species ($O_2(^1\Delta)$, $O_2(^1\Sigma)$, $O(^1D)$, $N_2(A)$ and $N(^2D)$ are metastable excited electronic states. $O(^3P)$ and $N(^4S)$ are the oxygen and nitrogen atom ground electronic states.

The production of species such as NO, NO_2, HNO_2, and HNO_3 is highly dependent on the production and subsequent chemistry of $N(^4S)$ and $N(^2D)$. Virtually all of the $N(^2D)$ enters into the two following reactions.

$$N(^2D) + O_2 \rightarrow NO + O \qquad (1)$$

$$N(^2D) + H_2O \rightarrow NH + OH \qquad (2)$$

(When an excited state is not indicated the ground state is assumed.) At altitudes above sea level reaction 1 is by far the dominant mechanism depleting the $N(^2D)$. At sea level altitudes, however, the water vapor density is large enough to make reaction 2 account for as much as half of the $N(^2D)$ depletion. The products of reaction 2 are uncertain but are probably as shown.[3] The introduction of NH adds even more uncertainty into the chemistry since very little is known about the reactions of this species. The rate coefficient of only the reaction

$$NH + NO \rightarrow \text{Products} \qquad (3)$$

has been measured[4] but the products are unknown. We had to estimate or guess the other reactions and rate coefficients involving NH.

The ground state nitrogen, $N(^4S)$, will primarily enter into the following reactions.

$$N + O_2 \rightarrow NO + O \qquad (4)$$

$$N + NO \rightarrow N_2 + O \qquad (5)$$

$$N + NO_2 \rightarrow N_2O + O \quad (6)$$

$$N + OH \rightarrow NO + H \quad (7)$$

$$N + HO_2 \rightarrow NO + OH \quad (8)$$

Reactions 4 through 8 are those mainly responsible for the conversion of the initially formed atomic nitrogen back to N_2 or to NO and N_2O.

The sum of the $N(^4S)$ and $N(^2D)$ formed initially is (from Table 1) 1.24 per ion-pair. To this must be added the N^+ (0.14 per ion-pair) which will react with air species to yield $N(^4S)$, $N(^2D)$, NO, NO_2 or N_2O. This 1.38 "odd nitrogen" per ion-pair is the pool from which N_2O and NO_x, where x = 1 or 2, will eventually be formed. The N_2O is extremely stable with regard to reactions with other neutral species. Some of the NO_x will continue to react according to the following major reactions

$$NO + O + M \rightarrow NO_2 + M \quad (9)$$

$$NO + O_3 \rightarrow NO_2 + O_2 \quad (10)$$

$$NO + HO_2 \rightarrow NO_2 + OH \quad (11)$$

$$O + NO_2 \rightarrow NO + O_2 \quad (12)$$

$$H + NO_2 \rightarrow NO + OH \quad (13)$$

$$NO + OH + M \rightarrow HNO_2 + M \quad (14)$$

$$NO_2 + OH + M \rightarrow HNO_3 + M \quad (15)$$

The above reactions will cause some of the NO_x to be converted to HNO_y, where y = 2 or 3.

Many of the reactions listed heretofore involve H, OH and HO_2 as reactants. Some of the "odd hydrogen" comes from reaction 2 and other neutral reactions. The bulk of the odd hydrogen, however, is generated by chemical evolution of the positive ions. Unless the electron density is extremely high (greater than about 10^{15} cm^{-3}) virtually all the initial ions undergo a complex evolution prior to recombination which yields ions of the form $H_3O^+ \cdot (H_2O)_n$, where n can be zero through four in our code and higher than four in the real world. Obviously at some point in this ion hydration scheme an H_2O is broken up and an OH radical released. When the $H_3O^+ \cdot (H_2O)_n$ recombines, either with an electron or with a negative ion, an H is released. This will generally combine with O_2 to form HO_2. Thus more than two odd hydrogen species are formed per ion pair (the odd hydrogen formed by reaction 2 must be added to those formed by the ion hydration and recombination).

These species, however, are not long-lived. Several processes act to reconstitute water vapor or H_2. The most important of these is the reaction

$$OH + HO_2 \rightarrow H_2O + O_2 \qquad (16)$$

This has a rather large rate coefficient at sea level densities ($\sim 10^{-10}$ cm^3/sec) and the size of this rate coefficient controls the amount of odd hydrogen present and causes it to decay rapidly when the ionizing source is turned off.

The amount and distribution of odd nitrogen species will greatly depend on the chemical scheme, the main features of which have been described above. The size of the radiation dose and its duration will also have an impact. If the dose is large enough, the air will be heated considerably.

Because of the size of reaction 16, the amount of the HNO_2 and HNO_3 formed by the above reaction scheme is minimal. For the radiation pulses characteristic of nuclear bursts, i.e., large doses of about a millisecond or less duration, we obtain at most 0.1 combined HNO_2 and HNO_3 produced per ion pair. In general, the shorter the pulse the less we obtain.

SECTION 3
OAK RIDGE EXPERIMENT

Oak Ridge National Laboratory conducted an experiment[5] in which a parcel of air was irradiated with a beam of 1.0 MeV electrons and the gas was periodically analyzed by infrared spectrophotometry. The dose rate was 1.73×10^{20} eV/min for an air volume of 3.80×10^{2} cm^3. This corresponds to an ionization rate of 2.2×10^{14} ion-pairs/cm^3-sec. This is less, by many orders of magnitude, than that experienced by a parcel of air close to but outside the nuclear fireball. The sample was, however, irradiated for up to 60 minutes or more and this is many orders of magnitude longer than the neutron and X-ray pulse from a nuclear weapon. The total integrated dose is of the order, or greater, than what might be expected in the nuclear case. The experiment showed that for a total dose of about 8×10^{16} ion-pairs/cm^3, there were 8×10^{16} cm^{-3} of HNO_3 formed and 2.7×10^{16} cm^{-3} of N_2O formed. The production of HNO_3 continued beyond that dose at a rate linear to the dose until all the water vapor was depleted. Beyond that point the HNO_3 disappeared rapidly and NO_2 was formed at the same rate as that of the HNO_3 depletion. When all the HNO_3 was gone the rate of NO_2 production per ion-pair slowed considerably. N_2O continued to be produced throughout the whole dose range but decreased somewhat at high integrated doses. No mention was made of HNO_2 and we assumed that none was observed. In a variation of the experiment NO_2 was initially added to the air sample. In that case no HNO_3 was produced and only about half the N_2O.

The nuclear cases of interest correspond to total doses which would not deplete all the H_2O. At doses such that the H_2O would be significantly depleted, the air temperature would become high enough to

thermally dissociate the N_2O and HNO_3 and cause the chemistry scheme to be different. In the experiment the irradiation was spread over a time long enough that cooling by the walls probably kept the air sample from getting significantly hotter than ambient.

Our multispecies chemical integration code using the neutral chemistry scheme described earlier predicted a much lower production rate for HNO_3 than was observed in this experiment. Since HNO_3 is a very efficient attacher of electrons, and since the value we calculate is far too low, we reviewed our chemistry looking for changes that would increase the HNO_3 production and bring it into agreement with the experiment. These revisions could impact the nuclear case significantly.

SECTION 4
ION-ION RECOMBINATION

It was noted earlier that the positive ions produced initially by the weapon radiation are transformed into ions of the type $H_3O^+ \cdot (H_2O)_n$. At sea level densities the electron attachment coefficient is very large (about 10^8 sec^{-1}) and unless the electron density is very high the electrons will attach before they recombine. The primary negative ion initially formed, O_2^-, will be involved in a complex chemical scheme in which it is transformed to NO_2^- and NO_3^-. Ions such as O_3^-, O_4^-, CO_3^-, CO_4^- and OH^- act as intermediates in this transformation. The NO_2^- and NO_3^- may also be hydrated, i.e., have one or more attached water molecules.

The products of the recombination of $H_3O^+ \cdot (H_2O)_n$ and NO_2^- and NO_3^- are unknown and we have heretofore assumed the following

$$H_3O^+ \cdot (H_2O)_n + NO_2^- \rightarrow H + NO_2 + (H_2O)_{n+1} \tag{17}$$

$$H_3O^+ \cdot (H_2O)_n + NO_3^- \rightarrow H + NO_3 + (H_2O)_{n+1} \tag{18}$$

The choice was arbitrary and could have been

$$H_3O^+ \cdot (H_2O)_n + NO_2^- \rightarrow HNO_2 + (H_2O)_{n+1} \tag{19}$$

$$H_3O^+ \cdot (H_2O)_n + NO_3^- \rightarrow HNO_3 + (H_2O)_{n+1} \tag{20}$$

In fact, from an energetic point of view, reactions 19 and 20 would be preferred. Under conditions which would allow all the ions to convert to those shown in the right-hand side of the above reactions, i.e., when the dose rate and electron density are small, we would expect a yield of about one HNO_2 or HNO_3 per ion pair just from reactions 19 and 20. This would certainly contribute greatly in the Oak Ridge experiment. In the nuclear case the dose rates and electron densities are much higher and the yield of HNO_2 and HNO_3 would be somewhat less.

In addition, when reactions 17 and 18 are used the free hydrogen released combines with O_2 to form HO_2 which then can react with OH by reaction 16. When reactions 19 and 20 are used instead of 17 and 18 the hydrogen atom is tied up in HNO_2 and HNO_3. These species can also react with OH to yield H_2O but with much smaller rates than with HO_2. This means the water vapor reformation will be slowed and the OH will be around longer. This should enhance the HNO_2 and HNO_3 production by reactions 14 and 15.

SECTION 5
NO_2 NEUTRAL CLUSTERS

Another change that was made in our chemistry scheme was that the species N_2O_5 and HO_2NO_2 were added. These species are formed in the following reactions

$$NO_2 + NO_3 + M \rightarrow N_2O_5 + M \qquad (21)$$

$$HO_2 + NO_2 + M \rightarrow HO_2NO_2 + M \qquad (22)$$

These species have been observed and measured rate coefficients for reactions 21 and 22 have been reported.[6,7] At temperatures above about 300 K the species N_2O_5 did not have much importance and we will therefore not discuss reaction 21 any further. The species HO_2NO_2 did have a significant effect. The only reported reactions involving this species are

$$OH + HO_2NO_2 \rightarrow \text{Products} \qquad (23)$$

$$O + HO_2NO_2 \rightarrow \text{Products} \qquad (24)$$

Reaction 24 has an activation energy of about 0.3 eV and is therefore not very important at ambient temperatures. In the nuclear case, however, it may be important under high dose conditions. We have assumed two channels for reaction 23 and divided the reported rate coefficient equally between them. The first channel yields HO_2 and HNO_3 as the products. The second yields $H_2O + O_2$ and NO_2 as the products. In the first case the rate coefficient is less than for the direct formation of HNO_3 from OH and NO_2

(reaction 15). In the second case the rate coefficient is much less than the direct reaction of OH and HO_2 (reaction 16). Thus having a substantial amount of the NO_2 and HO_2 tied up as HO_2NO_2 would decrease the rate formation of HNO_3 and the rate of reformation of water vapor. Reducing the rate of water reformation would, however, extend the longevity of OH and this would enhance the formation of both HNO_2 and HNO_3 by reactions 14 and 15. As it turns out the longer persistance of OH seems to dominate in the Oak Ridge experiment but in the nuclear case the net effect is minimal for a variety of reasons.

SECTION 6
CALCULATIONAL SIMULATION OF EXPERIMENT

We have run our multi-species chemical integration code to simulate the Oak Ridge experiment. Our code integrates the coupled rate equations for electrons, 27 neutral species, 27 positive ion species, and eleven negative ion species. The code contains over 450 reactions in addition to the two-body and three-body ion-ion recombination reactions. Many of the latter reactions are lumped together in our code. This is possible because we assume the same rate coefficient for all two-body recombination and similarly for all three-body recombination.

A constant ionization rate of 2.2×10^{14} ion-pairs/cm^3-sec was applied to air which contained about 0.1 percent H_2O by volume. The reaction scheme included reactions 25 and 26 rather than reactions 23 and 24 and also included HO_2NO_2 and N_2O_5. The code was run out to almost 5000 seconds which corresponded to a total dose rate of about 10^{18} ion-pairs/cm^3. The initial temperature was 298 K but the air was allowed to heat about 0.5 K per second to a maximum of 360K. It reached this maximum at a total dose of about 2.5×10^{16} ion-pairs/cm^3 or at about 120 seconds.

Our calculational results are in fair agreement with the experiment. Our HNO_3 production is about 0.6 per ion-pair and the HNO_2 production is 0.1 per ion-pair. This compares with a value of 1.0 for HNO_3 in the experiment and zero HNO_2. The N_2O production is in even better agreement. We obtained a value of 0.3 N_2O per ion-pair. The experimental value was 0.34.

About 80 to 90 percent of the HNO_3 is made, as expected, by reactions 15 and 20, i.e.,

$$OH + NO_2 + M \rightarrow HNO_3 + M$$

$$H_3O^+ \cdot (H_2O)_n + NO_3^- \rightarrow HNO_3 + (H_2O)_{n+1}$$

The remainder is made by other reactions, including reaction 23. A significant amount of HNO_3 is destroyed by the reactions

$$NO_2^- + HNO_3 \rightarrow NO_3^- + HNO_2 \qquad (25)$$

$$e + HNO_3 \rightarrow NO_2^- + OH \qquad (26)$$

Both of these are reactions for which the rate coefficients have been measured and it is reaction 26 which makes HNO_3 potentially important in the nuclear case.

The main production of HNO_2, surprisingly, is neither reaction 14 nor 19 but reaction 25. The reaction

$$NO^+ \cdot (H_2O)_3 + H_2O \rightarrow H_3O^+ \cdot (H_2O)_2 + HNO_2 \qquad (27)$$

also contributes. The main destruction mechanism of HNO_2 is

$$OH + HNO_2 \rightarrow H_2O + NO_2 \qquad (28)$$

The main production of N_2O is through reaction 6, i.e.,

$$N + NO_2 \rightarrow N_2O + O$$

As the total dose increases beyond about 2×10^{16}, the increased temperature makes its effect felt. The HO_2NO_2 concentration drops significantly as does the OH and HO_2 concentrations. The HO_2NO_2 is very weakly bound and an increase in temperature of just 50 K causes the large drop in its concentration. The OH can react more rapidly with the free HO_2 and disappears more quickly. This reduces the production of HNO_3 and causes the HNO_3 concentrtion to drop dramatically to insignificance. (This suggests that the experiment did not involve any temperature increase.)

The HNO_2 and N_2O production per ion-pair, however, remain about the same as before at these large doses. Before the temperature increases, the calculated HNO_3 production is about 60 percent of what was obtained in the experiment. We consider this fair agreement but more HNO_3 production is needed in the calculation to get better agreement. There are a number of possible ways this may occur. One way is if the amount of ground state and excited nitrogen atoms produced during the initial energy deposition is more than we have assumed. The values given in Table 1 are the result of calculations using both theoretical and measured cross sections and a number of uncertainties are involved. It is quite possible more odd nitrogen is formed than is shown in Table 1.

Another possibility is that the rate coefficient we have used for reaction 16, i.e.,

$$OH + HO_2 \rightarrow H_2O + O_2$$

is too large. This is a measured value but it seems to be pressure dependent and this is not yet understood. The uncertainty in this rate is as much as a factor of two.[6,7]

Still another possiblity to increase the HNO_3 production is that there are reactions which convert HNO_2 to HNO_3. Some possible reactions which accomplish this are

$$HNO_2 + O + M \rightarrow HNO_3 + M \tag{29}$$

$$HNO_2 + HO_2 \rightarrow HNO_3 + OH \tag{30}$$

$$HNO_2 + H_2O_2 \rightarrow HNO_3 + H_2O \tag{31}$$

SECTION 7
NUCLEAR EFFECTS CALCULATIONS

Both a set of sequential bursts and a single burst (larger than any of the sequential bursts) were calculated to simulate the effect on the atmosphere of the prompt ionizing radiation from a nuclear burst (X-rays, gammas and neutrons). Depending on the type of weapon and its burst height, the prompt radiation can be deposited in the air anywhere from microseconds to even milliseconds. We assumed a time variation such that about 80 percent of the radiation is deposited in the air by 10^{-5} seconds for the multiburst calculations. This is fairly typical of many weapons detonated close to the ground. In this set of runs eight bursts, thirty seconds apart and each having a total ionization of 6×10^{15} ion-pairs, were calculated. Both the new and old chemistry were used. In none of these calculations was the temperature allowed to rise. The single burst, for which the total ionization was 6×10^{16} ion-pairs, was also calculated with both the old and the new chemistry. The temperature was allowed to rise as the energy was deposited and for 6×10^{16} ion-pairs the temperature rise is about 350 K. In addition the bulk of the ionization (about 80 percent) was produced by about 10^{-4} seconds rather than by 10^{-5} seconds as in the multiburst calculations.

In the multiburst calculations, i.e., the set of eight consecutive bursts, the HNO_3 production was, surprisingly, the same for the old chemistry and the new. After the first burst the HNO_3 production was about 0.05 per ion-pair which quickly rose with subsequent bursts to about 0.10 HNO_3 molecule per ion-pair. Apparently the tying up of the NO_2 in HO_2NO_2 decreased the HNO_3 producton as much as the tying up of the HO_2.

In addition, during the time of major ion-ion recombination the negative ion distribution has not yet developed fully and NO_2^- is the major ion rather than NO_3^-. Thus recombination with $H_3O^+(H_2O)_n$ will yield HNO_2 rather than HNO_3.

The HNO_2 production is, therefore, larger than the HNO_3 production. For the new chemistry runs it is about 0.16 per ion pair and for the runs with the old chemistry it is about 0.09.

The HNO_3 production is much less than that for the calculation described in the last section, i.e., when the ionization dose is spread out over a couple of minutes, and the HNO_2 production is greater. One of the reasons for this is NO_2^- is the major negative ion during the major deionization phase. Another reason is that the OH disappears shortly after the ionization pulse decays while NO_2 takes time to appear. The overlap between the two is the only time HNO_3 can form by OH + NO_2 combination and this overlap time is short. On the other hand NO is formed almost immediately when the ionization pulse is turned on so that NO + OH combination is favored. Still another reason is that in the nuclear case the electron density is large enough to compete with the negative ions in neutralizing the positive ions. Thus reaction 26 contributes less to production of HNO_3 than in the experiment.

We see that the timing of the ionization pulse is a critical factor in the production of HNO_3. For a given total ionization the longer it takes the energy to be deposited the more HNO_3 will be produced. The single pulse calculations for a total ionization of 6×10^{16} ion-pairs and a 10^{-4} second ionization pulse should give the same answers for HNO_3 production as the multiburst calculations since the total ionization is about the same and the combined pulse time is also the same. The HNO_3 production was, in fact, much smaller. The value was about 0.03 HNO_3 per ion-pair for the new chemistry and about 0.02 for the old. The HNO_2 production was about 0.08 and 0.05, respectively. This is a factor of about

three, for the HNO_3, and a factor of two, for the HNO_2, less than the multiburst results. The difference is due to the fact that in the single burst calculations the gas temperature was allowed to rise as energy was deposited. This 300 or so degree rise in temperature effects the HNO_3 production in at least two ways. The first way, already noted in a previous section, is to prevent a significant amount of HO_2NO_2 from being formed. The second way is to reduce the value of the ion-ion recombination coefficient. This rate coefficient is assumed to have a $T^{-2.5}$ dependence and doubling the temperature reduces the coefficient by about a factor of six. This means that electrons will compete more successfully with the negative ions for positive ions with which to recombine. This, in turn, means that reactions 19 and 20 will produce less HNO_2 as well as HNO_3.

To sum up our results regarding HNO_3, the nuclear case will not produce nearly as much per ion-pair as was produced in the experiment. This is primarily due to the fact that in the nuclear case the bulk of the ionization is produced very quickly. If the temperature of the gas is raised significantly by the energy deposition the yield of HNO_3 per ion pair will be reduced further.

The attachment rate due to attachment to O_2 at sea level is between 5×10^7 and 10^8 sec^{-1}. The attachment rate coefficient of HNO_3 is 5×10^{-8} cm^3/sec at 300 K. (The rate coefficient may decrease with increasing temperature but this is unknown.) Therefore concentrations of HNO_3 of about 10^{15} cm^{-3} or more could change the total attachment significantly. With a value of 0.03 HNO_3 per ion-pair this would require a total ionization of about 3×10^{16} ion-pairs or more for the HNO_3 attachment to dominate the attachment. Ionization doses of this magnitude are quite possible within a kilometer or so of a large yield burst.

The value of the HNO_3 production could be significantly larger than the value of 0.03 obtained in the single burst calculation. Types of

weapons which radiate the bulk of their energy over millisecond or greater times would yield more HNO_3. The production of HNO_3 could also be increased by the reaons given in the last section, i.e., if the amount of odd nitrogen produced initially per ion pair is larger than we have shown in Table 1, or if the rate coefficient for reaction 22 is smaller than we have used, or if an efficient mechanism exists which converts HNO_2 to HNO_3. This last possibility could be quite important since in the nuclear cases we have calculated, the HNO_2 production was two to three times the HNO_3 production.

The amount of N_2O produced in all the nuclear cases we calculated was about 0.18 per ion-pair. For N_2O to compete as an efficient attacher of electrons the N_2O must be in excited vibrational states corresponding to the gas being heated to near 1000K or so. This requires an ionization dose of between 10^{17} and 2×10^{17} ion-pairs. Under these conditions the N_2O can become a significant electron attacher.

The only other species produced in the single burst nuclear case in quantities large enough to be an appreciable attacher of electrons is H_2O_2. It is produced at the rate of about 0.05 per ion-pair. The reaction

$$e + H_2O_2 \rightarrow H_2O + O^- \qquad (32)$$

is energetically very nearly resonant so if this reaction has a large rate coefficient the reverse reaction should also have a large coefficient. This is not the case.[8] However, as is the case with other molecules such as N_2O, the rate may increase dramatically when the H_2O_2 is in an excited vibrational state. Thus when the deposition is large enough to heat the gas significantly, H_2O_2 may become an important electron attacher.

SECTION 8
BOMBLIGHT EFFECTS

For a certain time after burst the fireball will radiate a considerable amount of energy in the visible and ultraviolet regions of the spectrum. This energy can impact the chemistry through photoexcitation, photodissociation and photodetachment processes.

Although the temperature of the fireball during the radiative growth phase can be very high (many eV), the radiation does not escape the fireball. It is not until what is called "second maximum" in the radiative output that the bulk of the radiative energy escapes. For large yield bursts this occurs at a time of the order of a second and the radiating temperature is about 6000 K. Since this is the same radiating temperature as the sun we can obtain the photochemical rates at the point in question by taking those derived for sunlight at the top of the atmosphere and multiply by the ratio of the solid angle subtended by the fireball to the solid angle subtended by the sun. This yields for the photochemical rate, k

$$k = 4.6 \times 10^4 \left(\frac{R}{d}\right)^2 k_s \quad \text{sec}^{-1} \tag{33}$$

where R is the radius of the fireball, d is the distance from the burst point, and k_s is the corresponding sunlight photochemical rate. k and k_s are in units of sec^{-1}. For a nominal large yield burst the radius at first maximum is about 0.6 km. For d = 1.2 km we have

$$k = 1.2 \times 10^4 \, k_s \quad \text{sec}^{-1} \tag{34}$$

We wish to know whether the photodetachment rate caused by these processes can ever dominate the ionization rate produced by the delayed gamma radiaion from the weapon. To do this we use the detachment rate coefficients obtained by equation 34 for the various negative ions present and the negative ion distribution and obtain a value for the overall detachment of about 250 times the negative ion concentration, M^-. Virtually all of the detachment comes from the species O_2^-, O^-, NO_2^- and NO_3^-. For steady-state conditions, the value of M^- is given by[7]

$$M^- = \sqrt{q/\alpha_i} \quad \text{cm}^{-3} \tag{35}$$

where q is the value of the ionizing source in cm^{-3}/sec and α_i is the ion-ion recombination rate in cm^3/sec. The value of q at which the production of electrons by detachment is equal to the direct production by the ionizing source is given by

$$q = \frac{6.3 \times 10^4}{\alpha_i} \quad \text{cm}^{-3}/\text{sec} \tag{36}$$

For larger values of q the direct ionization will dominate the detachment. Using a value of 1.4×10^{-6} cm^3/sec for α_i we obtain a value from Equation 36 of about 5×10^{10} cm^{-3}/sec. At about a second and a distance of 1.2 kilometers from the burst the ionization rate due to delayed gamma radiation is more than two orders of magnitude larger than 5×10^{10} cm^{-3}/sec.[9] Thus, bomblight photodetachment will not be an important factor in determining the electron density when compared to direct delayed gamma ionization. This has been confirmed by calculations using our chemistry code.

The bomblight can also indirectly affect the electron density via photodissociation. The primary candidates for these effects are O_3 and NO_2. When an O_3 photodissociates an atomic oxygen and an $O_2(^1\Delta)$ are formed and both of these can chemically detach O_2^- and O^- via the reactions

$$O_2^- + O_2(^1\Delta) \rightarrow O_2 + O_2 + e \tag{37}$$

$$O_2^- + O \rightarrow O_3 + e \tag{38}$$

$$O^- + O_2(^1\Delta) \rightarrow O_3 + e \tag{39}$$

$$O^- + O \rightarrow O_2 + e \tag{40}$$

The photodissociation of NO_2 produces an atomic oxygen and an NO molecule. The NO can detach O^- by the reaction

$$O^- + NO \rightarrow NO_2 + e \tag{41}$$

More importantly the decrease in O_3 and NO_2 concentrations as a result of photodissociation causes an affect in the steady-state negative ion distribution. The transformation of initially produced O^- and O_2^- to more strongly bound negative ions, involves a number of intermediate negative ions such as O_3^- and CO_3^-. O_3 is a vital reactant in the formation of these species. NO_2 is involved in the further transformation of these negative ions to NO_2^- and NO_3^-, ions which are not as easily detached as O^- and O_2^-. A significant reduction of O_3 and NO_2, particularly O_3, would slow down this evolution of O^- and O_2^- to NO_2^- and NO_3^- and would change the steady-state negative ion distribution to one in which the concentrations of O^- and O_2^- would be larger than before. This would, of course, increase both the photo and chemical detachment.

The sunlight photodissociation rates of O_3 and NO_2 are both about 10^{-2} sec^{-1}. Multiplying this by a factor given in Equation 34 yields

$$k = 120 \ sec^{-1} \tag{42}$$

Adding this destruction mechanism to our code for O_3 and NO_2 did make an appreciable effect in the concentrations of these species, particularly for O_3. We also added the increased direct photodetachment by bomblight of all negative ions. The combined effects did increase the detachment significantly but still not enough to have detachment compete with the delayed gamma ionizing source. Thus the electron density was not affected significantly.

In addition, the effect of intervening O_3 and NO_2 in reducing the photon flux at the point in question was not included. O_3, in particular, has a rather large absorption cross-section and an average O_3 density of only 10^{13} cm^{-3} or less between the fireball edge and the point in question would severly attenuate the dissociating light flux. Our calculations indicate enough O_3 would be present to reduce the photon flux at least an order of magnitude or more.

If we were to move in closer to the fireball edge the effects of photodissociation of O_3 and NO_2 would increase. However, we would be encountering gas which would be significantly heated by the greater inital energy deposition and also by the outgoing shock wave. In this gas thermal dissociation would become important and would outweigh the photodissociation.

In summary, it does not seem that bomblight will have any first order effects on the electron densities in the air surrounding the burst.

SECTION 9
CONCLUSIONS

Although the production of HNO_3 in slowly irradiated air is large the yield is considerably less for the nuclear burst case where the irradiation time is typically quite short. Enough HNO_3, however, is produced in the nuclear case to make it potentially important as an attacher of electrons. In addition, there are a number of uncertainties in the formation processes leading to HNO_3 production that might lead to an even higher production of HNO_3.

Significant quantities of N_2O are formed in the nuclear case but N_2O is only an important attacher of electrons in gas which has been heated to about 1000K or so. This might be accomplished by the initial energy deposition and the outgoing shock wave in a limited region near the burst.

Bomblight effects on the electron density are at most marginal. Bomblight effects might be important for low yield weapons for which the radiating temperature at second maximum is significantly larger than 6000 K. However, these effects would be limited to times much less than a second and to distances from the fireball edge of a fireball radius or less. For a low yield weapon this would be of the order of 50 meters or less.

REFERENCES

1. Gilmore, F. R., Private communication, 1980 and Preliminary Revised Production Rate Distribution for Bombarded Air, letter dated 28 May 1974, R & D Associates.

2. Meyers, B. F., and M. R. Schoonover, UV Photon and Electron Deposition in the Atmosphere, DNA 4068F, Science Applications Inc., August 1976 and Electron Energy Degradation in the Atmosphere, DNA 3513T, Science Applications Inc., January 1975.

3. Black, G., Private communication, 1980.

4. Hampson, R. F., Chemical Kinetics and Photochemical Data Sheets for Atmospheric Reactions, Department of Transportation, Report No. FAA-EE-80-17, April 1980.

5. Jones, A. R., Radiation-Induced Reactions in the N_2 - O_2 - H_2O System, Radiation Research, 10, 655 (1959).

6. Baulch, et. al., Evaluated Kinetic and Photochemical Data for Atmospheric Chemistry, J. Phys. Chem. Ref. Data, 11, 327 (1982).

7. DeMore, W. B., Chemical Kinetics and Photochemical Data for Use in Stratospheric Modeling: Evaluation Number 5, Jet Propulsion Laboratory Publication 82-57, 1982.

8. Albritton, D. L., Ion-Neutral Reaction-Rated Constants Measured in Flow Reactors Through 1977, Atomic Data and Nuclear Tables 22, 1 (1978).

9. Knapp, W. S. and K. Schwartz, Aids for the Study of Electromagnetic Blackout, DNA 3449H, General Electric TEMPO, February 1975.

DISTRIBUTION LIST

DEPARTMENT OF DEFENSE

Defense Advanced Rsch Proj Agency
ATTN: GSD, R. Alewene
ATTN: STO, W. Kurowski

Defense Communications Agency
ATTN: Code 230
ATTN: Code 205
ATTN: J300 for Yen-Sun Fu

Defense Communications Engineer Center
ATTN: Code R410, N. Jones
ATTN: Code R123, Tech Lib

Defense Intelligence Agency
ATTN: DB-4C
ATTN: DB, A. Wise
ATTN: DT-1B
ATTN: Dir
ATTN: DC-7B

Defense Nuclear Agency
ATTN: STNA
ATTN: RAEE
ATTN: NAWE
ATTN: RAAE, P. Lunn
ATTN: NATF
4 cy ATTN: STTI/CA
3 cy ATTN: RAAE

Defense Technical Info Ctr
12 cy ATTN: DD

Dep Under Secy of Defense, Comm, Cmd, Cont & Intell
ATTN: Dir of Intelligence Sys

Field Command/DNA, Det 1
Lawrence Livermore Lab
ATTN: FC-1

Field Command, Defense Nuclear Agency
ATTN: FCPR
ATTN: FCTXE
ATTN: FCTT, W. Summa

Interservice Nuclear Weapons School
ATTN: TTV

Joint Chiefs of Staff
ATTN: C3S
ATTN: C3S Eval Office, HD00

Joint Data System Support Ctr
ATTN: G510, G. Jones
ATTN: C-312, R. Mason
ATTN: G510, P. Bird

Joint Strat Tgt Planning Staff
ATTN: JPPFD
ATTN: JPSS
ATTN: JPTM
ATTN: JLKS
ATTN: JLK, DNA Rep

National Security Agency
ATTN: B-43, C. Goedeke
ATTN: W-36, O. Bartlett

DEPARTMENT OF DEFENSE (Continued)

Under Secy of Def for Rsch & Engrg
ATTN: Strat & Space Sys, OS
ATTN: Strat & Theater Nuc For, B. Stephan

WWMCCS System Engineering Org
ATTN: R. Crawford

DEPARTMENT OF THE ARMY

Army Logistics Management Ctr
ATTN: DLSIE

Assistant Chief of Staff for Automation & Comm
ATTN: DAMO-C4, P. Kenny

Atmospheric Sciences Laboratory
ATTN: DELAS-EO, F. Niles

BMD Advanced Technology Ctr
ATTN: ATC-R, W. Dickinson
ATTN: ATC-T, M. Capps

BMD Systems Command
ATTN: BMDSC-LEE, R. Webb
2 cy ATTN: BMDSC-HW

Dep Ch of Staff for Ops & Plans
ATTN: DAMO-RQC, C2 Div

Harry Diamond Laboratories
ATTN: DELHD-NW-P, 20240
ATTN: DELHD-NW-R, R. Williams, 22000

US Army Chemical School
ATTN: ATZN-CM-CS

US Army Comm-Elec Engrg Instal Agency
ATTN: CC-CE-TP, W. Nair

US Army Communications Command
ATTN: CC-OPS-WR, H. Wilson
ATTN: CC-OPS-W

US Army Communications R&D Command
ATTN: DRDCO-COM-RY, W. Kesselman

US Army Foreign Science & Tech Ctr
ATTN: DRXST-SD

US Army Material Command
ATTN: DRCLDC, J. Bender

US Army Nuclear & Chemical Agency
ATTN: Library

US Army Satellite Comm Agency
ATTN: Doc Control

US Army TRADOC Sys Analysis Actvy
ATTN: ATAA-TCC, F. Payan, Jr
ATTN: ATAA-PL
ATTN: ATAA-TDC

DEPARTMENT OF THE NAVY

Joint Cruise Missiles Project Ofc
ATTN: JCMG-707

Naval Air Systems Command
ATTN: PMA 271

Naval Electronic Systems Command
ATTN: Code 501A
ATTN: Code 3101, T. Hughes
ATTN: PME 117-20
ATTN: PME 106-4, S. Kearney
ATTN: PME 117-211, B. Kruger
ATTN: PME 117-2013, G. Burnhard
ATTN: PME 106, F. Diederich

Naval Intelligence Support Ctr
ATTN: NISC-50

Naval Research Lab
ATTN: Code 4720, J. Davis
ATTN: Code 7500, B. Wald
ATTN: Code 4780
ATTN: Code 4700
ATTN: Code 4187
ATTN: Code 7950, J. Goodman
ATTN: Code 6700
ATTN: Code 4108, E. Szuszewicz

Naval Space Surveillance System
ATTN: J. Burton

Naval Surface Weapons Center
ATTN: Code F31

Naval Telecommunications Command
ATTN: Code 341

Ofc of the Deputy Chief of Naval Ops
ATTN: NOP 981N
ATTN: NOP 941D
ATTN: NOP 654, Strat Eval & Anal Br

Office of Naval Research
ATTN: Code 412, W. Condell

Strategic Systems Project Office
ATTN: NSP-43, Tech Lib
ATTN: NSP-2141
ATTN: NSP-2722

Theater Nuc Warfare Prj Office
ATTN: PM-23, D. Smith

DEPARTMENT OF THE AIR FORCE

Air Force Geophysics Laboratory
ATTN: OPR-1
ATTN: LYD, K. Champion
ATTN: CA, A. Stair
ATTN: LIS, J. Buchau
ATTN: R. Babcock
ATTN: R. O'Neil

Air Force Satellite Ctrl Facility
ATTN: WE

Air Force Weapons Laboratory
ATTN: SUL
ATTN: NTN

DEPARTMENT OF THE AIR FORCE (Continued)

Air Force Space Technology Ctr
ATTN: YH

Air Force Wright Aeronautical Lab/AAAD
ATTN: W. Hunt
ATTN: A. Johnson

Air Logistics Command
ATTN: OO-ALC/MM

Air University Library
ATTN: AUL-LSE

Asst Chief of Staff, Studies & Analysis
ATTN: AF/SASC, C. Rightmeyer

Ballistic Missile Office/DAA
ATTN: ENSN
ATTN: SYC, D. Kwan
ATTN: ENSN, W. Wilson

Deputy Chief of Staff, Research, Dev, & Acq
ATTN: AFRDQI
ATTN: AFRDS, Space Sys & C3 Dir
ATTN: AFXOKCD
ATTN: AFXOKS
ATTN: AFXOKT

Electronic Systems Div
ATTN: SCS-2, G. Vinkels
ATTN: SCS-1E

Foreign Technology Div
ATTN: NIIS, Library
ATTN: TQTD, B. Ballard

Rome Air Development Center
ATTN: EEP, J. Rasmussen
ATTN: EEPS, P. Kossey

Rome Air Development Center
ATTN: TSLD
ATTN: OCSA, R. Schneible
ATTN: OCS, V. Coyne

Space Command
ATTN: DC, T. Long

Strategic Air Command
ATTN: DCX
ATTN: DCZ
ATTN: NRI/STINFO Library
ATTN: XPFC
ATTN: XPFS
ATTN: XPQ

DEPARTMENT OF ENERGY

Department of Energy, GTN
ATTN: DP-233

OTHER GOVERNMENT AGENCIES

US Department of State
ATTN: PM/STM

Central Intelligence Agency
ATTN: OSWR/SSD for K. Feuerpfetl

OTHER GOVERNMENT AGENCIES (Continued)

National Oceanic & Atmospheric Admin
ATTN: R. Grubb
ATTN: F. Fehsenfeld

National Bureau of Standards
ATTN: Sec Officer for R. Moore

Institute for Telecommunications Sciences
ATTN: A. Jean
ATTN: L. Berry
ATTN: W. Utlaut

DEPARTMENT OF ENERGY CONTRACTORS

EG&G, Inc
ATTN: J. Colvin
ATTN: D. Wright

Univ of CA, Lawrence Livermore National Lab
ATTN: Tech Info Dept Lib

Los Alamos National Lab
ATTN: D. Sappenfield
ATTN: G-6, E. Jones

Sandia National Laboratories
ATTN: D. Dahlgren
ATTN: Space Project Div
ATTN: Tech Lib 3141
ATTN: D. Thornbrough
ATTN: Org 1250, W. Brown
ATTN: Org 1231, R. Backstrom

Sandia National Laboratories
ATTN: T. Cook
ATTN: B. Murphey
ATTN: R. Grossman

DEPARTMENT OF DEFENSE CONTRACTORS

Aerospace Corp
ATTN: S. Mewaters

Aerospace Corp
ATTN: J. Kluck
ATTN: I. Garfunkel
ATTN: D. Olsen
ATTN: J. Straus
ATTN: R. Slaughter
ATTN: T. Salmi
ATTN: V. Josephson
ATTN: K. Cho
ATTN: D. Whelan

Analytical Systems Engineering Corp
ATTN: Security

Analytical Systems Engineering Corp
ATTN: Radio Sciences

Austin Research Assoc
ATTN: J. Thompson
ATTN: B. Moore
ATTN: M. Sloan
ATTN: J. Uglum

BDM Corp
ATTN: L. Jacobs
ATTN: T. Neighbors

DEPARTMENT OF DEFENSE CONTRACTORS (Continued)

Berkeley Rsch Associates, Inc
ATTN: J. Workman
ATTN: S. Brecht

Boeing Co
ATTN: MS 8K-85, Dr S. Tashird

Boeing Co
ATTN: G. Hall

BR Communications
ATTN: J. McLaughlin

University of California at San Diego
ATTN: H. Booker

California Research & Tech, Inc
ATTN: M. Rosenblatt

Charles Stark Draper Lab, Inc
ATTN: D. Cox
ATTN: J. Gilmore
ATTN: A. Tetewski

Communications Satellite Corp
ATTN: G. Hyde
ATTN: D. Fang

Computer Sciences Corp
ATTN: F. Eisenbarth

Cornell University
ATTN: D. Farley, Jr
ATTN: M. Kelly

Electrospace Systems, Inc
ATTN: H. Logston

EOS Technologies, Inc
ATTN: B. Gabbard
ATTN: W. Lelevier

General Electric Co
ATTN: R. Juner
ATTN: A. Steinmayer
ATTN: C. Zierdt

General Electric Co
ATTN: G. Millman

General Research Corp
ATTN: B. Bennett

GTE Communications Products Corp
ATTN: H. Gelman

GTE Government Systems Corp
ATTN: R. Steinhoff

Honeywell, Inc
ATTN: A. Kearns, MS924-3
ATTN: G. Terry, Avionics Dept

Horizons Technology, Inc
ATTN: R. Kruger

HSS, Inc
ATTN: D. Hansen

DEPARTMENT OF DEFENSE CONTRACTORS (Continued)

IBM Corp
ATTN: H. Ulander

Institute for Defense Analyses
ATTN: E. Bauer
ATTN: H. Wolfhard
ATTN: J. Aein

ITT Corp
ATTN: G. Wetmore

ITT Corp
ATTN: Technical Library

JAYCOR
ATTN: H. Dickinson

JAYCOR
ATTN: J. Sperling

Johns Hopkins University
ATTN: K. Potocki
ATTN: T. Evans
ATTN: J. Newland
ATTN: R. Stokes
ATTN: J. Phillips
ATTN: C. Meng

Kaman Sciences Corp
ATTN: E. Conrad

Kaman Tempo
ATTN: DASIAC

Kaman Tempo
ATTN: DASIAC
ATTN: B. Gambill

Litton Systems, Inc
ATTN: B. Zimmer

Lockheed Missiles & Space Co, Inc
ATTN: Dept 60-12
2 cy ATTN: D. Churchill, Dept 62-A1

Lockheed Missiles & Space Co, Inc
ATTN: J. Kumer
ATTN: R. Sears

MIT Lincoln Lab
ATTN: D. Towle
ATTN: V. Vitto
ATTN: N. Doherty

M/A Com Linkabit Inc
ATTN: I. Jacobs
ATTN: H. Van Trees
ATTN: A. Viterbi

Magnavox Govt & Indus Electronics Co
ATTN: G. White

Maxim Technologies, Inc
ATTN: J. Marshall
ATTN: E. Tsui
ATTN: R. Morganstern

McDonnell Douglas Corp
ATTN: W. Olson

DEPARTMENT OF DEFENSE CONTRACTORS (Continued)

Meteor Communications Corp
ATTN: R. Leader

Mission Research Corp
ATTN: G. McCartor
ATTN: F. Gugliano
ATTN: Tech Library
ATTN: F. Fajen
ATTN: R. Bogusch
ATTN: R. Hendrick
ATTN: D. Knepp
ATTN: S. Gutsche
ATTN: R. Dana
ATTN: C. Lauer
ATTN: R. Bigoni
2 cy ATTN: M. Scheibe
5 cy ATTN: Doc Control

Mitre Corp
ATTN: A. Kymmel
ATTN: G. Harding
ATTN: C. Callahan

Mitre Corp
ATTN: W. Hall
ATTN: W. Foster
ATTN: M. Horrocks

Pacific-Sierra Research Corp
ATTN: E. Field, Jr
ATTN: F. Thomas
ATTN: H. Brode, Chairman SAGE

Pennsylvania State University
ATTN: Ionospheric Research Lab

Photometrics, Inc
ATTN: I. Kofsky

Physical Dynamics, Inc
ATTN: E. Fremouw
ATTN: J. Secan

Physical Research, Inc
ATTN: J. Devore
ATTN: J. Thompson

Physical Research, Inc
ATTN: R. Deliberis
ATTN: T. Stephens
ATTN: K. Schueter

R&D Associates
ATTN: M. Gantsweg
ATTN: C. Greifinger
ATTN: F. Gilmore
ATTN: H. Ory
ATTN: R. Turco
ATTN: W. Wright
ATTN: W. Karzas
ATTN: G. Stcyr
ATTN: P. Haas

R&D Associates
ATTN: B. Yoon

Rand Corp
ATTN: B. Bennett

DEPARTMENT OF DEFENSE CONTRACTORS (Continued)

Rand Corp
ATTN: C. Crain
ATTN: E. Bedrozian
ATTN: P. Davis

Riverside Research Institute
ATTN: V. Trapani

Rockwell International Corp
ATTN: S. Quilici

Rockwell International Corp
ATTN: R. Buckner

Science Applications, Inc
ATTN: M. Cross

SRI International
ATTN: C. Rino
ATTN: J. Petrickes
ATTN: D. Neilson
ATTN: R. Livingston
ATTN: M. Baron
ATTN: R. Leadabrand
ATTN: W. Chesnut
ATTN: W. Jaye
ATTN: G. Smith
ATTN: A. Burns
ATTN: G. Price
ATTN: R. Tsunoda

Stewart Radiance Lab
ATTN: R. Huppi

DEPARTMENT OF DEFENSE CONTRACTORS (Continued)

Science Applications, Inc
ATTN: C. Smith
ATTN: D. Sachs
ATTN: D. Hamlin
ATTN: E. Straker
ATTN: L. Linson

Swerling, Manasse & Smith, Inc
ATTN: R. Manasse

Toyon Research Corp
ATTN: J. Garbarino
ATTN: J. Ise

TRW Electronics & Defense Sector
ATTN: R. Plebuch

Utah State University
Attention Sec Control Ofc for
ATTN: A. Steed
ATTN: D. Burt
ATTN: K. Baker, Dir Atmos & Space Sci
ATTN: L. Jensen, Elec Eng Dept

Visidyne, Inc
ATTN: H. Smith
ATTN: J. Carpenter
ATTN: W. Reidy
ATTN: O. Shepard

END

FILMED

6-85

DTIC